

# High precision thermal, structural and optical analysis of an external occulter using a common model and the general purpose multi-physics analysis tool Cielo

Claus Hoff<sup>a</sup>, Eric Cady<sup>b</sup>, Mike Chainyk<sup>b</sup>, Andrew Kissil<sup>b</sup>, Marie Levine<sup>b</sup>, Greg Moore<sup>b</sup>

<sup>a</sup>Cielo Engineering Software LLC,  
2436 Burson Rd, Topanga, CA 90290

<sup>b</sup>Jet Propulsion Laboratory, California Institute of Technology,  
4800 Oak Grove Dr, Pasadena, CA 91109

## ABSTRACT

The efficient simulation of multidisciplinary thermo-opto-mechanical effects in precision deployable systems has for years been limited by numerical toolsets that do not necessarily share the same finite element basis, level of mesh discretization, data formats, or compute platforms. Cielo, a general purpose integrated modeling tool funded by the Jet Propulsion Laboratory and the Exoplanet Exploration Program, addresses shortcomings in the current state of the art via features that enable the use of a single, common model for thermal, structural and optical aberration analysis, producing results of greater accuracy, without the need for results interpolation or mapping. This paper will highlight some of these advances, and will demonstrate them within the context of detailed external occulter analyses, focusing on in-plane deformations of the petal edges for both steady-state and transient conditions, with subsequent optical performance metrics including intensity distributions at the pupil and image plane.

**Keywords:** Multi-physics, integrated modeling, steady state and transient thermal analysis, finite elements, parallel computing, high precision thermal deformations

## 1. INTRODUCTION

In spite of continued advances in the field of numerical analysis, the efficient simulation of complex thermo-opto-mechanical systems has remained a challenge due to a number of nontrivial factors. Disparate solution time scales, varying levels of spatial and feature discretization, and the combination of linear (structural) and nonlinear (heat transfer) effects have conspired to drive computational tool development largely along separate discipline-specific paths. The task of integrating the pieces is generally left to the ingenuity and creativity of the analyst who then still must contend with larger issues such as integration into a controlled optical system.

Cielo is an open, object-based, multidisciplinary, high-performance compute environment that addresses these disparities, and enables a single common-model approach consisting of thermal, structural, and optical interface attributes. Funded through the Jet Propulsion Laboratory's Research and Technology Development program, and with recent generous support from the Exoplanet Exploration Program, Cielo is MATLAB<sup>®</sup><sup>1</sup> hosted, leverages client/server high-performance parallel computing, and implements native heat transfer, structural, and optical aberration capabilities. By virtue of its back-end parallel compute server, Cielo enables extensible MATLAB-hosted solutions for models that range into the hundreds of thousands of radiation exchange surfaces and millions of structural degrees of freedom.

Though clearly motivated by challenges in precision deployable systems, Cielo is also an entirely general-purpose finite element code. The external occulter analysis described here was thus an opportunity not only for benchmarking within the context of an extremely relevant analysis task, but also to demonstrate its suitability for future missions. Within the context of such systems, the traditional structural, thermal, optical process (STOP) with commercial off-the-shelf

(COTS) tools involves at least two disparate models. A coarse finite element model is built to run a thermal solver. All COTS thermal solvers available today have model size limits. The resulting temperature field is mapped to a finer mesh for the structural solver. In-house MATLAB scripts pull out results data of the structural solver to feed optical codes: either in-house or COTS. The process is labor intensive, error prone and inaccurate. Cielo works from a common model with multi-physics attributes for thermal and structural analysis including optical element definitions to calculate optical aberrations. The ASCII data input format of the common model is based on Nastran, which is the standard structural solver in the aerospace industry. An overview of the process using Cielo versus traditional COTS tools is illustrated in Fig. 1. JPL is using the NX CAE<sup>2</sup> tools from Siemens. The CAD model is meshed in NX CAE calling NX Thermal<sup>3</sup> with a coarse mesh, mapping the temperatures to a finer mesh and calling NX Nastran<sup>4</sup>.

Cielo starts with the mesh of a Nastran structural model. The user adds thermal attributes with help from the NX CAE pre-processor. Conduction, capacitance, MLI blankets, radiation surfaces, thermal loads and boundary conditions are created on the structural mesh. Cielo performs steady state and transient thermal analysis including view factor calculations, radiation exchange, solar loads in orbit, conduction, and capacitance. Without temperature mapping, structural analysis is performed to determine thermal deformations at any time station. If optical elements are present, optical aberrations are calculated. Cielo permits switching back and forth to COTS tools at any time during the analysis. Temperature fields from Cielo can be written out to run a Nastran structural analysis, and Cielo can read temperature fields from other solvers. This allows a direct comparison and concurrent analysis with COTS tools.

In summary, Cielo offers reduction in turn around time by orders of magnitude, higher accuracy with double precision arithmetic throughout the entire process, and can afford large model sizes at practical wall clock times. In addition, Cielo offers easy integration of third party software and extension via MATLAB hosting. Cielo's technology readiness level has been grown over the years and demonstrated on several large scale production models, see Chainyk et al.<sup>5</sup> and Jordan et al.<sup>6</sup>

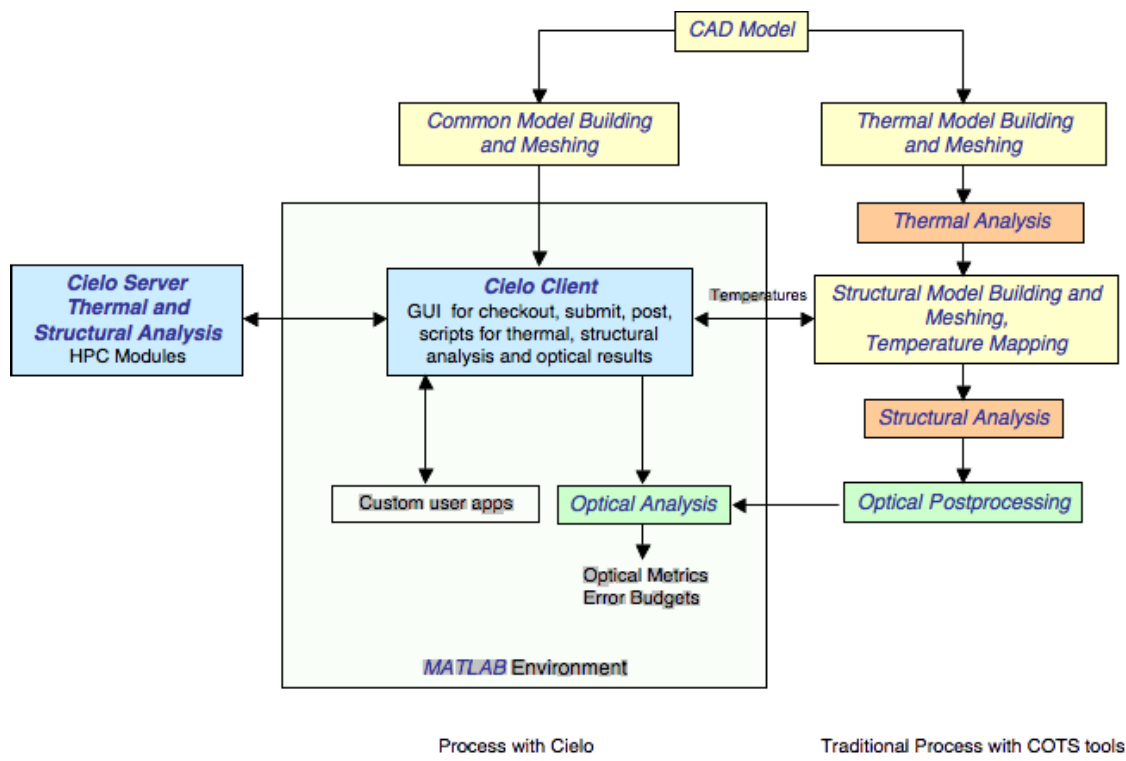


Figure 1. Cielo versus the traditional process in thermal-structural-optical analysis

## 2. EXTERNAL OCCULTER CONCEPT AND DESIGN REQUIREMENTS

An occulter is a large, flat spacecraft which, when flown in conjunction with a telescope, would allow imaging of objects near stars at very high contrasts ( $\sim 10^{10}$ ) and small angular separations ( $\sim 100\text{mas}$ ). In particular, they are being designed for direct imaging of exoplanets. This is done by positioning the occulter between the telescope and the target star, suppressing the starlight at the telescope aperture. The occulter is placed at a distance such that the angular size of the occulter allows light from planets orbiting the star to pass unhindered. (See Fig. 2 for a diagram of the system.)

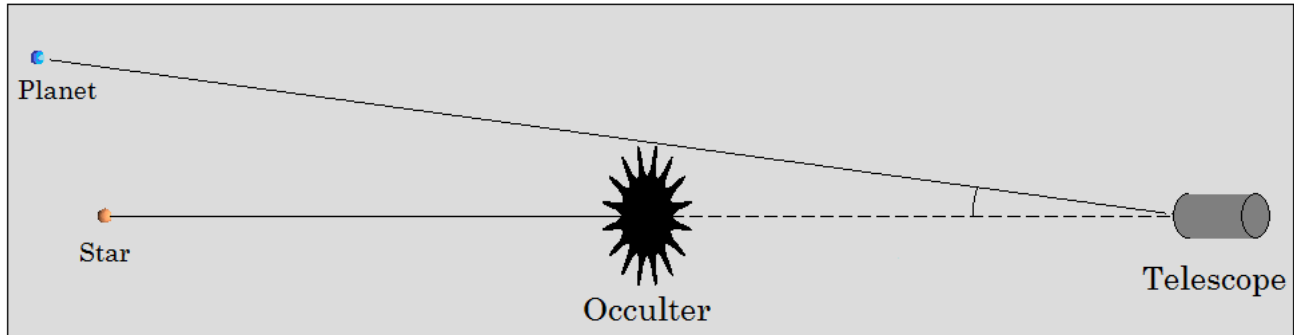


Figure 2. The concept of an external occulter: a spacecraft is placed at a distance where it blocks starlight while allowing planet light to pass.

The edge of the occulter is shaped—generally into repeating structures known as petals—such that diffraction from the edge ensures the shadow is sufficiently deep over a broad spectral band. (See for example Vanderbei et al. 2007<sup>7</sup> for more on the design of the edges.) As this shaped edge is the reason that the starlight can be suppressed to such a high degree, it also must be manufactured and maintained to high accuracy: scales from millimeters to tens of microns, depending on the specific error.<sup>8,9</sup>

The particular occulter we are simulating is part of the Occulting Ozone Observatory ( $\text{O}_3$ ) mission concept,<sup>10,11</sup> which would use an occulter with a low-cost 1.1m telescope to obtain photometric data in up to 8 bands from atmospheres of nearby terrestrial planets, including one band which could indicate the presence of ozone. The occulter itself is 30m across with 24 petals, 7.25m long each, and with a solid central region providing a location for the spacecraft bus and solar panels. It sits at 38,960km from the telescope and nominally it provides  $10^{10}$  suppression across the 250-550nm band at 75mas and beyond, though it can be moved to half the distance and provide this suppression over the 550-1100nm band beyond 150mas. The shape is shown in Fig. 3. The occulter and the telescope are designed to be small enough to fit in one launch bay. The occulter is packed in a 4m diameter cylinder shape, the petals are wrapped around a circular truss, unfurl and fold down when the truss opens, as shown in Fig. 4.

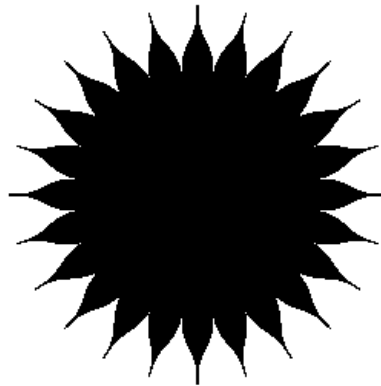


Figure 3. Shape of the  $\text{O}_3$  occulter, which produces a dark shadow at the pupil plane of the telescope.

One operational constraint for occulter, particularly important for thermal considerations, is the sun angle. The sun can never be allowed to hit the face of the occulter during an observation, as this would reflect light off the face and ruin the suppression being provided. In fact, it should not even be allowed to approach too closely to an edge-on configuration; 80-85° is generally an upper limit. This means that (1) one face of the occulter is continuously dark, while the other is continuously illuminated, and (2) the shadowing of petals by the central spacecraft bus depends on the sun angle, becoming most extreme as the sun angle approaches 90°. In particular, sun angles near 90° result in a configuration with sections of 1-3 petals being in continuous shadow, with the remainder of the face in continuous sunlight. Determining the effects of this shadowing on the precision shape of the edge, and whether operational fixes such as a slow spin on the occulter can mitigate them, is a key question that integrated modeling can address.

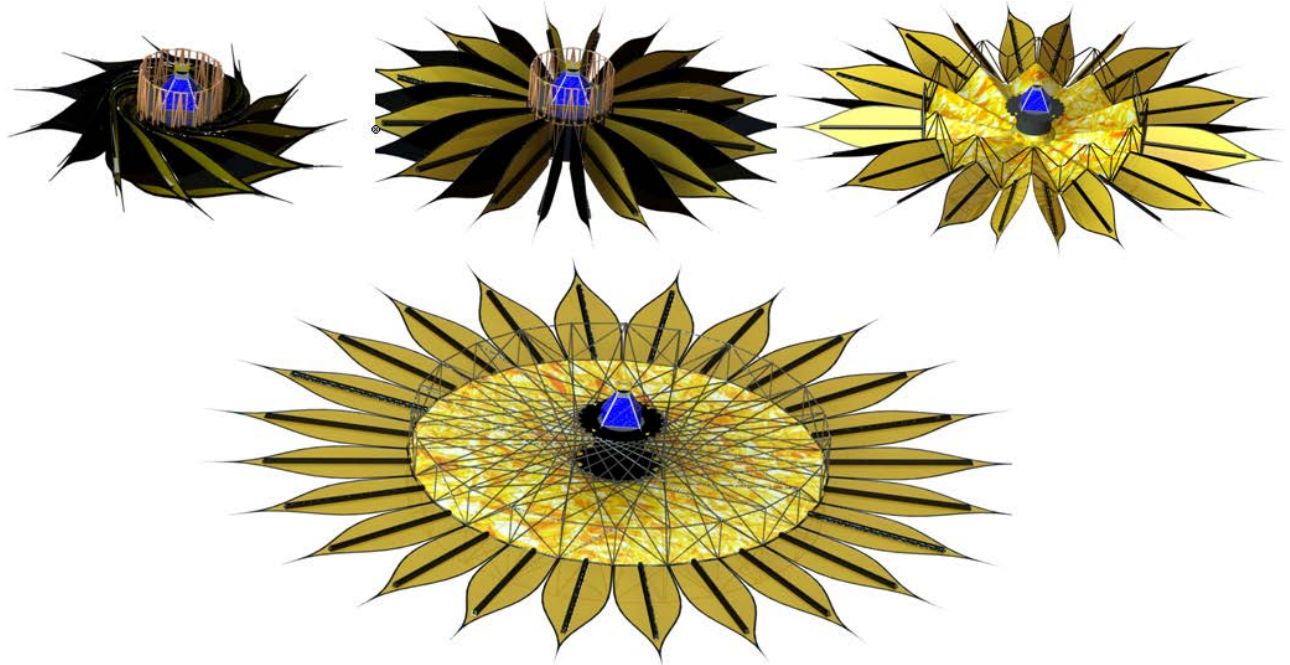


Figure 4. O<sub>3</sub> occulter deployment. Petals wrapped around a central truss unfurl when the truss opens, to a 30m diameter operating configuration.

### 3. BUILDING A COMMON MODEL

Initial studies had been performed using highly detailed structural models with mesh densities driven primarily by curve-fitting requirements along the petal edges. Several heat transfer studies had also been performed using models that had necessarily been simplified to accommodate commercial tool limitations, and the results mapped to the detailed structural mesh. Given this non-optimal situation, and the desire to eventually perform parametric studies that may prove to be dependent on local effects, the detailed structural mesh was used as a basis for the combined thermal/structural Cielo model, eliminating the need for all future mapping exercises, and thus greatly improving turnaround time.

The Nastran structural model does not contain a mesh for the membrane-like cover of the occulter because it is structurally not important. The mass of the cover is accounted for in the structural model as a nonstructural mass on the underlying petal frames and trusses. The primary function of the cover is to block the star light. The cover consists of 3 thin kapton layers for redundant protection against micro meteorites. A multi-layer insulator (MLI) blanket is added to the petals to keep the underlying frame warm while it is exposed to the sun. With help from the NX FEMAP<sup>12</sup> pre-processor, we add a flat mesh on the telescope side to model the thermal behavior of the cover. From the star side to the telescope side, the cover consists of a radiation surface towards the star with high absorptivity and emissivity (cavity 1), a thin low conductivity shell, a blanket across the petal areas, and a radiation surface towards the telescope with low absorptivity and emissivity (cavity 2), see Fig. 5. A sun “element” is also included in cavity 1. The blanket elements

model the MLI with an effective emissivity between two close surfaces. The cover is connected to the petal frames and to the central spacecraft with fasteners or glue modeled with high conductivity rods.

The petal frames (edges, battens and spines) consist of T300 laminate and M55J composite material with a low coefficient of thermal expansion (CTE). The petal edges have two layers; the upper layer is machined to precision. The petal frame is modeled with tiny shell elements which are paved with radiation surface elements on both sides and associated with cavity 1. Modeling the radiation exchange effect of the tiny shell elements turns out to be necessary to get quality temperature distribution at the petal edges which, in turn, influence edge deformations. The load carrying circular frame and other stabilizing trusses are modeled with bar elements. The bars also have radiation surfaces in cavity 1 receiving sun loads and radiating to space. Because the bars are very thin, their radiation exchange with other surfaces is neglected. All shells and bars have conduction and capacitance properties. The final model is shown in Figures 5 and 6. Blue lines are bars and rods, gray lines are shell elements.

The temperature dependent conductivity of the M55 composite material is taken into account in thermal steady state and transient analysis. Overall the model has about 200k radiation surfaces and 170k thermal dof.

The structural model has about 1M dof. For the structural analysis in Cielo, the model does not need to be altered. Temperature solutions are taken directly without mapping. Thermal and structural solution steps are user-specified using Nastran-style subcases. Cielo activates elements based on analysis type and available material properties. For example, the cover has thermal properties but no structural properties and is therefore ignored in structural analysis. The user can request diagnostics to see which elements have been selected in an analysis step.

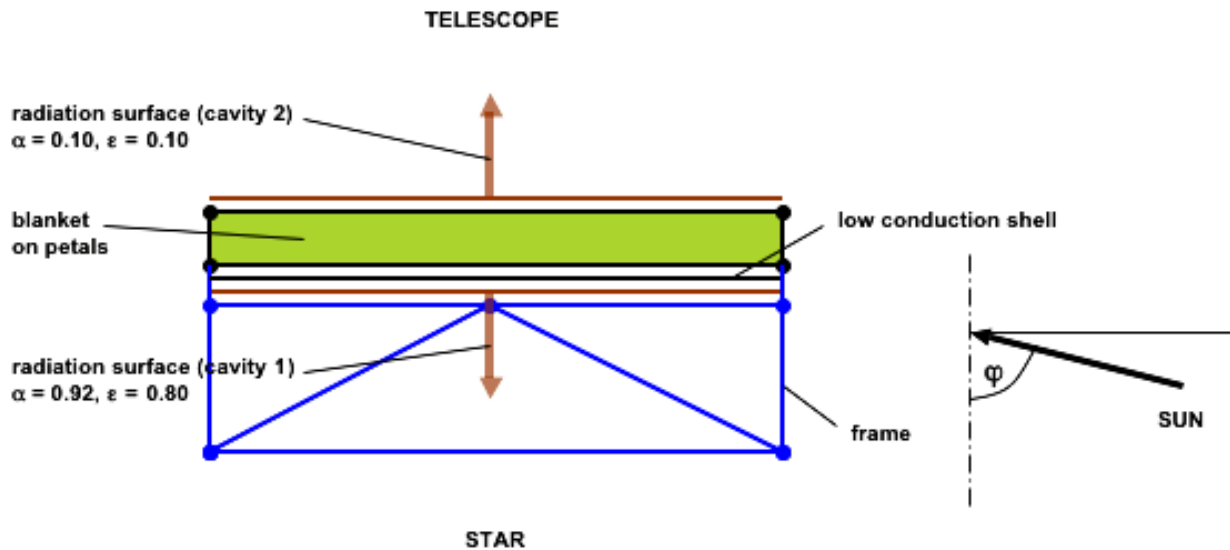


Figure 1. Schematic composition of the occulter cover for thermal analysis

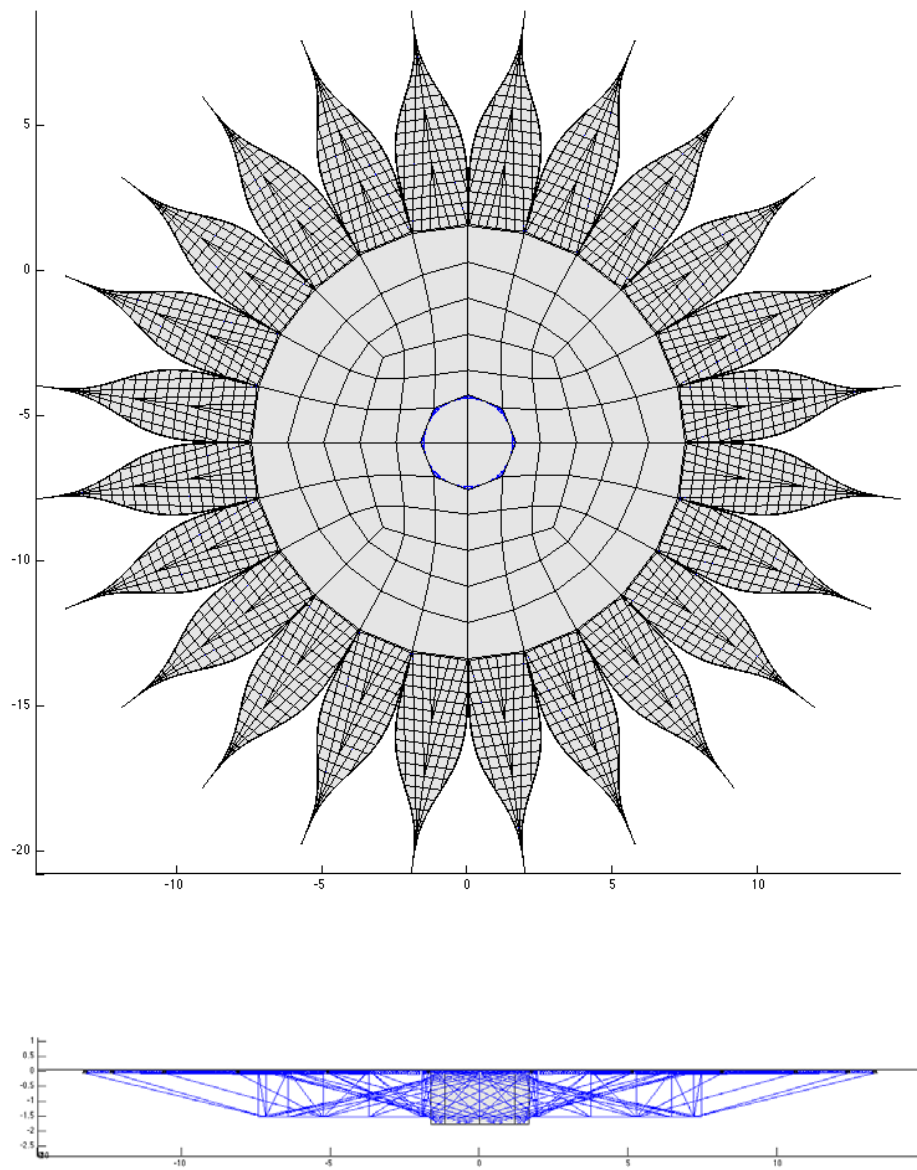
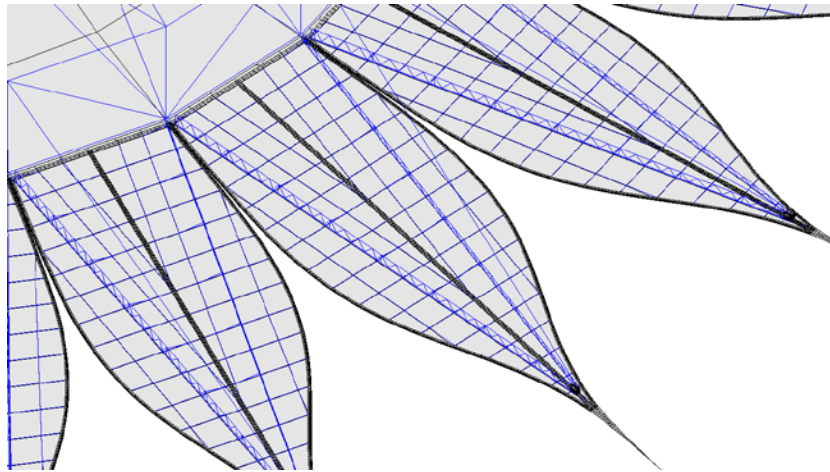
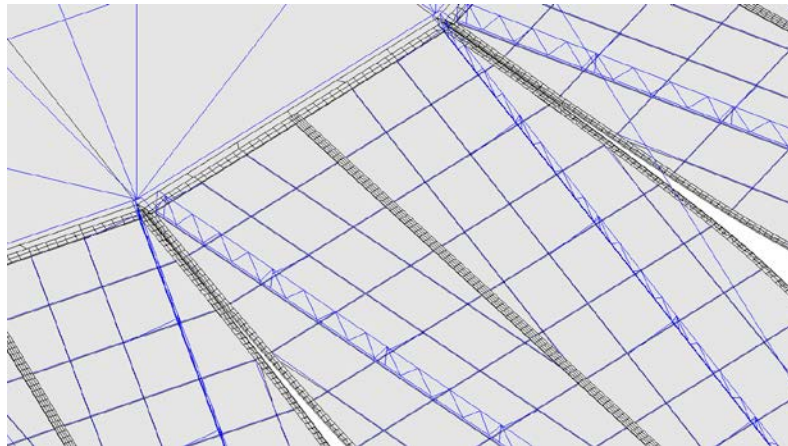


Figure 2. Occulter model, plan form (view from the telescope) and side on



Shell elements  
displayed with  
gray lines, bar  
elements with  
blue lines



T-section of two  
layer composite  
frame modeled with  
shell elements and  
including intralayer  
radiation exchange.

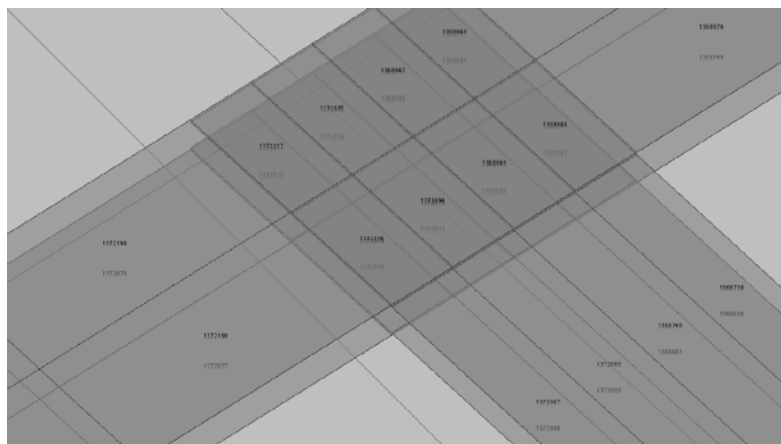


Figure 3. Details of the petals

## 4. INTEGRATED THERMAL- STRUCTURAL- OPTICAL ANALYSIS

### 4.1 Steady state analysis

Though Cielo scales extremely well when run on large symmetric multiprocessor parallel architectures, due to cost and schedule constraints all analyses were carried out with the remote compute server running locally on an Intel i7 dual core (four thread total) MacBook Pro. Though detailed view factor calculations for the 200k elements takes several hours of wall clock time on this hardware, the turnaround can be reduced to a matter of minutes with sufficient processing power. Subsequent nonlinear thermal analysis runs can restart from an existing database, benefitting from a reuse of previously-computed view factors. In Fig. 8, temperature distributions are shown for the sun shining at an 85° sun angle and straight on to petal 19 leaving petal 7 cold due to the shade of the spacecraft. The petals are numbered counter clockwise starting at noon.

A thermal analysis with a much coarser model was performed using the COTS tool NX Thermal, see Thomson et al.<sup>13</sup>. The model size had to be restricted due to size limits in the software and to keep run times practical. We have used the NX Thermal temperature results from smaller component models to verify material parameters and compare with Cielo's results. With the fine mesh at the critical petal edges, 400 grids along the perimeter of one petal, Cielo is able to model high resolution localized temperature variations and resulting deformations. NX Thermal produces a much coarser temperature field along the edges skipping 20 elements compared to Cielo.

The temperature field is directly applied to calculate thermal deformations, see Fig. 8. The deformations along the edges of all 24 petals is plotted, see Fig. 8. The maximum displacement of 2.e-4 m occurs at the tip of petal 7 and is in good agreement with results from NX Nastran when the temperature field from Cielo is imposed.

There are a few specialized approaches<sup>7,14</sup> to modeling propagation past an occulter. (Given that the edge must be specified at the level of tens of microns, using FFTs on a grid across the occulter's face would require prohibitively large matrices.) In this case, to determine the electric field past the perturbed occulter, we use the integral formulation outlined in Dubra and Ferrari 1999,<sup>14</sup> which integrates solely along the edge. In the output from the thermo-mechanical model, only the coordinates of the outermost points along the edge of the model are used. These points are projected into the plane perpendicular to the optical axis of the telescope—an approximation, but a very good one for the small deviations here—and these form a new edge which can be integrated to determine the level of starlight suppression provided by the occulter.

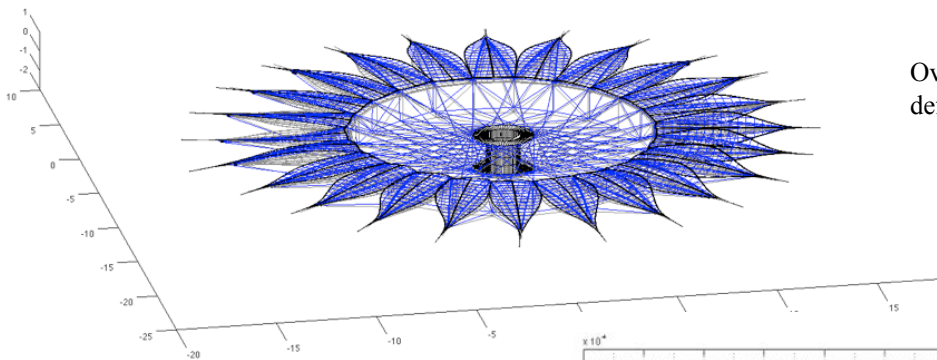
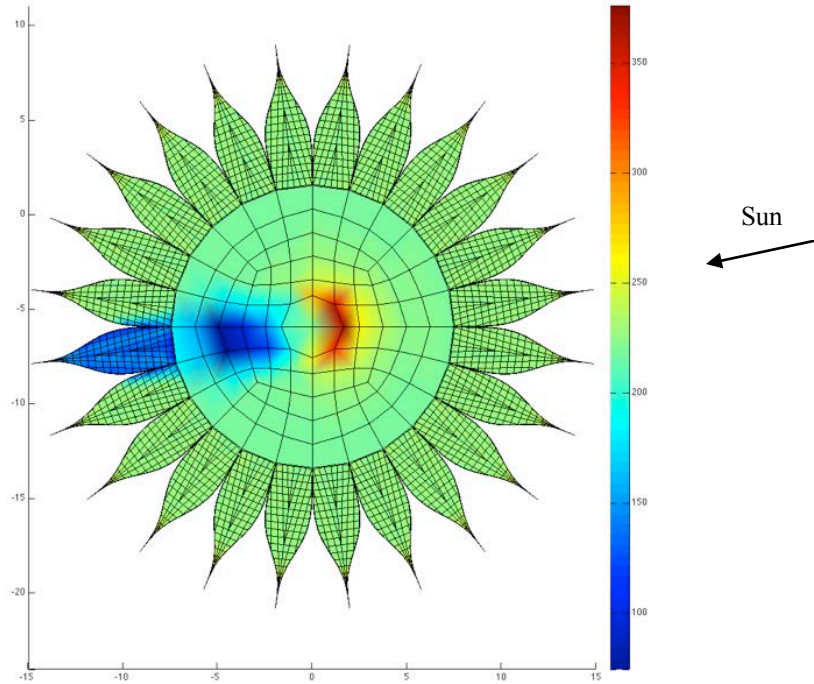
To test the performance of the occulter at its expected bounds of performance, the occulter was allowed to equilibrate to steady-state with an 85° sun angle. The resulting edge deformations were then run through the propagation code. Figure 9 shows pupil- and image-plane intensity profiles in the absence of thermal deformations at 250nm and 400nm; Figure 10 shows the same wavelengths, but with the sun incident at the oblique angle. The change is significant, though not show stopping, and suggests that testing methods of potentially mitigating the effects of large thermal variations would be worthwhile.

### 4.2 Transient analysis

The occulter may rotate around the telescope- star axis with 2 revolutions per hour in operating conditions to smooth local disturbances of the petal edges. The transient effects during rotation need to be investigated. First, we determine the thermal inertia of the system with a theoretical experiment. Starting with a converged steady state solution, we turn off the sun load and run a transient analysis to see when the temperature distribution becomes uniform or close to uniform. An hour after the sun load is turned off, the cold petal in the shadow of the spacecraft is still slightly cooler than the other petals. It can be concluded that with 2 revolutions per hour we will always have slight periodic temperature variations calling for a full transient analysis.

The thermal transient analysis in Cielo for one revolution took about 6 days wall clock time on the laptop. The transient effects after one revolution are illustrated in Figure 11.

Steady state temperatures  
 $t_{min}/t_{max} = 74.36/375.93 \text{ K}$



Overall thermal deformations

Total petal edge thermal deformations  
(counterclockwise beginning at noon)

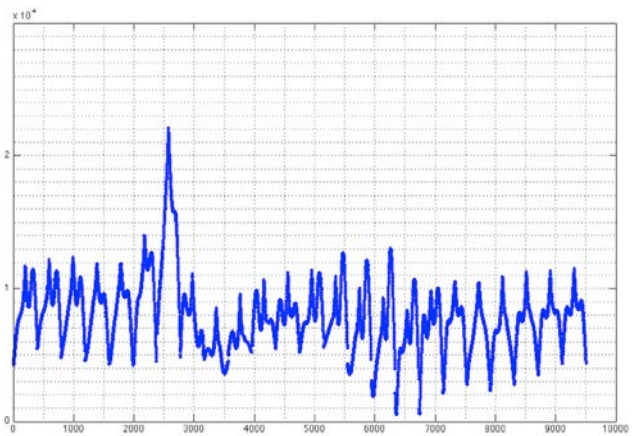


Figure 4. Steady state temperatures for  $85^\circ$  sun angle shining against the axis of petal 19 (counting from noon counter clockwise), and corresponding thermal deformations

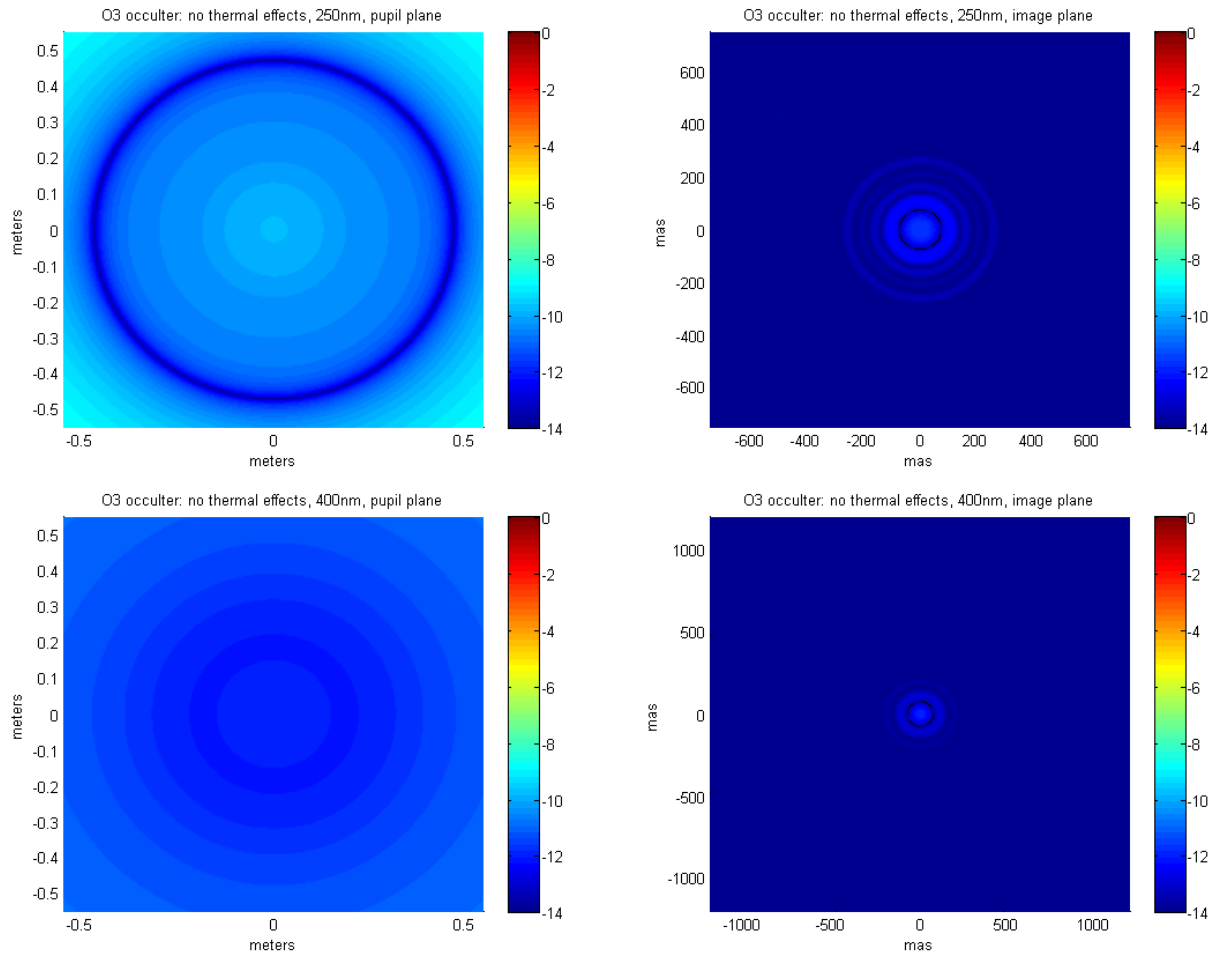


Figure 9: *Left.* The residual intensity across the telescope aperture in the absence of thermally-induced deformations, at  $\lambda = 250\text{nm}$  (top) and  $400\text{nm}$  (bottom). *Right.* Intensity in the image plane of the telescope at  $\lambda = 250\text{nm}$  (top) and  $400\text{nm}$  (bottom); the dashed circle has a radius of  $75\text{mas}$ .

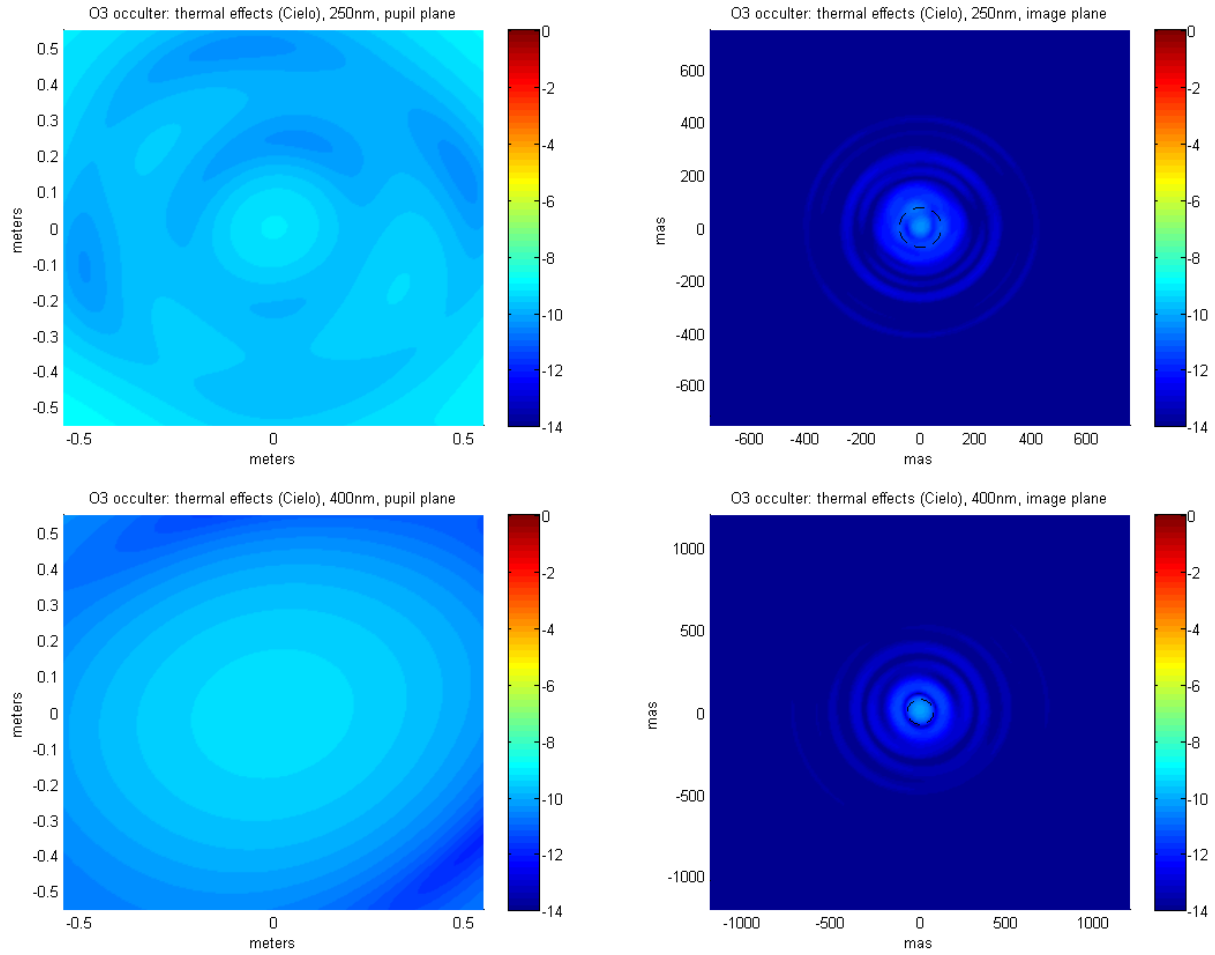
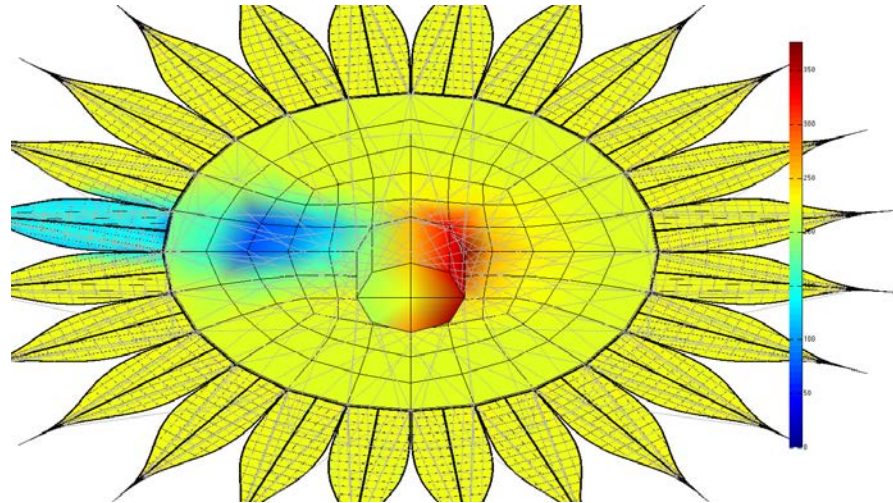


Figure 10: *Left.* The residual intensity across the telescope aperture with an  $85^\circ$  sun angle, at  $\lambda = 250\text{nm}$  (top) and  $400\text{nm}$  (bottom). *Right.* Intensity in the image plane of the telescope at  $\lambda = 250\text{nm}$  (top) and  $400\text{nm}$  (bottom); the dashed circle has a radius of  $75\text{mas}$ .

Steady state temperatures at  $t = 0$  (initial conditions)



Temperatures after one revolution at  $t = 30$  min.

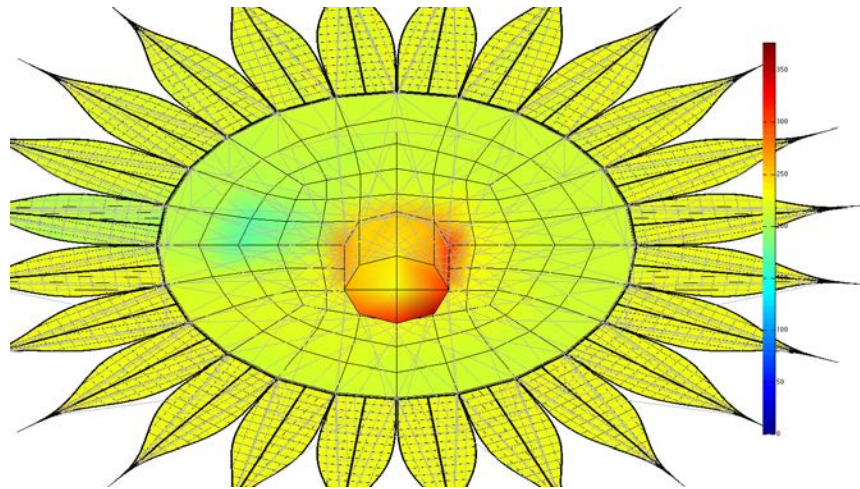


Figure 51. Thermal transient analysis starting with temperatures from steady state at  $t = 0$  and after one revolution at  $t = 30$  min.

## 5. CONCLUSIONS AND PLANS

We have demonstrated an integrated and seamless end-to-end thermal-structural-optical analysis on a common model of large size ( $> 200k$  radiation surfaces) using one software environment throughout. The Cielo software provides unique technologies making the simulation of models feasible which could not be handled in the past because of their size. We have shown reasonable wall clock times on a multithread laptop computer for these large models. With adequate hardware (32 to 128 processors), turnaround time can be reduced to a matter of hours or even minutes.

The current application is a technology demonstrator that points the way towards more efficient creation of multidisciplinary models. The high-performance aspect allows a greater degree of interactivity that will permit identification of modeling weaknesses, and efficient exploration of design alternatives. MATLAB hosting facilitates integration with other technologies and disciplines, as witnessed by the optical post-processing phases.

It is hoped that opportunities for subsequent parameter studies to cover various operational scenarios can be performed. The effects of varying sun illumination angle ( $30^\circ$  to  $85^\circ$ ), star shade angular velocities, and optimal material selections could be used to fine-tune system performance, increasing the range of available targets. In summary, the combination of the Cielo framework, and the ability to integrate externally-provided analytical tools via the MATLAB hosting layer, provides a robust platform for closed-loop optical performance optimization.

## ACKNOWLEDGEMENTS

The research was carried out at the Jet Propulsion Laboratory, California Institute of Technology, under a contract with the National Aeronautics and Space Administration.

## REFERENCES

- [1] MATLAB, see <http://www.mathworks.com/products/matlab/>
- [2] NX CAE, see [http://www.plm.automation.siemens.com/en\\_us/products/nx/simulation/](http://www.plm.automation.siemens.com/en_us/products/nx/simulation/)
- [3] NX Thermal, see [http://www.mayahtt.com/index.php?option=com\\_content&task=view&id=90&Itemid=295](http://www.mayahtt.com/index.php?option=com_content&task=view&id=90&Itemid=295)
- [4] NX Nastran, see [http://www.plm.automation.siemens.com/en\\_us/products/nx/simulation/nastran/index.shtml](http://www.plm.automation.siemens.com/en_us/products/nx/simulation/nastran/index.shtml)
- [5] Chainyk, M., Hoff, C., Larour, E., Moore, G., Schiermeier, J., "A thermo/opto/mechanical testbed validation using Cielo," Proc. SPIE 7071, 70710F (2008).
- [6] Jordan, E.O., Chainyk, M., Habbal, F., Hoff, C., Levine, M., Moore, G., "Thermo/opto/mechanical analysis of large apertures for exoplanet detection using Cielo," Proc. SPIE 7440, 74400U (2009)
- [7] Vanderbei, R., Cady, E., and Kasdin, N., "Optimal occulter design for finding extrasolar planets." *The Astrophysical Journal* **665**, 794-798 (2007).
- [8] Dumont, P., Shaklan, S., Cady, E., Kasdin, J., and Vanderbei, R., "Analysis of external occulters in the presence of defects," Proc. SPIE 7440, 744008 (2009).
- [9] Shaklan, S. B., Noecker, M. C., Glassman, T., Lo, A. S., Dumont, P. J., Kasdin, N. J., Cady, E. J., Vanderbei, R., and Lawson, P. R., "Error budgeting and tolerancing of starshades for exoplanet detection," Proc. SPIE 7731, 77312G (2010).
- [10] Kasdin, N. J., Spergel, D. N., Lisman, P. D., Shaklan, S. B., Savransky, D., Cady, E., Vanderbei, R., Thomson, M. W., Martin, S. R., Balasubramanian, K., Pravdo, S. H., Sato, Y., and Fujii, Y. "O<sub>3</sub>: The Occulting Ozone Observatory," in *[Bulletin of the American Astronomical Society]* (Jan. 2010).
- [11] Savransky, D., Spergel, D. N., Kasdin, N. J., Cady, E. J., Lisman, P. D., Pravdo, S. H., Shaklan, S. B., and Fujii, Y. "Occulting ozone observatory science overview," Proc. SPIE 7731, 77312H (2010).
- [12] NX FEMAP, see [http://www.plm.automation.siemens.com/en\\_us/products/velocity/femap/](http://www.plm.automation.siemens.com/en_us/products/velocity/femap/)
- [13] Thomson, M.W., Lisman, P.D., Helms, R., Walkemeyer, P., Kissil, A., Polanco, O., Lee, S.-C., "Starshade design for occulter based exoplanet missions," Proc. SPIE 7731, 773153 (2010).
- [14] Dubra, A. and Ferrari, J.A. "Diffracted field by an arbitrary aperture," *American Journal of Physics* **67**, 87-92 (1999).